

# INVERSE MODELLING TO OBTAIN HEAD MOVEMENT CONTROLLER SIGNAL

Won Soo Kim, Sang Hyo Lee\*,  
Blake Hannaford & Lawrence Stark

Neurology Unit, 481 Minor Hall,  
University of California, Berkeley, CA, 94720

20<sup>th</sup> Annual Conference on Manual Control  
June 1984

## ABSTRACT

Experimentally obtained dynamics of time-optimal, horizontal head rotations have previously been simulated by a sixth order, non-linear model driven by rectangular control signals. EMG recordings have aspects which differ in detail from the theoretical rectangular pulsed control signal. We have obtained control signals for time-optimal as well as sub-optimal horizontal head rotations by means of a newly developed inverse modelling procedure. With experimentally measured dynamical data serving as the input, this procedure inverts the model to produce the neurological control signals driving muscles and plant. The relationships between these controller signals, and EMG records should contribute to our understanding of the neurological control of movements.

Acknowledgements: NIH Training grant in Systems and Integrative Biology (BH); Nasa-Ames cooperative agreement NCC-2-86. S.H.L. is partially supported by a grant from the Ministry of Education, Korea.

## INTRODUCTION

Head movements are similar to arm movements about the elbow in dynamics and time scales (Lehman 1983) and are of interest because of their interactions with eye movements, posture, and perception. Zangemeister, et. al., 1981a-e, have studied head movements and their involvement in shifts of gaze, the eye's position in space. They have also quantified the dynamics of time-optimal horizontal head rotations in terms of the peaks of the dynamical variables position, velocity, and acceleration and plotted them in the Main Sequence diagram to show the relationship between dynamics and movement magnitude

Interest in the control mechanisms involved in head movements has lead to the study of the electromyographic activity of neck muscles involved in these movements (Zangemeister, Stark, Meienberg, & Waite & Stark, Hannaford et al. 1983) and to efforts to model the system.

\* On Leave: Department of Electronics Engineering, Kwang Woon University, Seoul, Korea

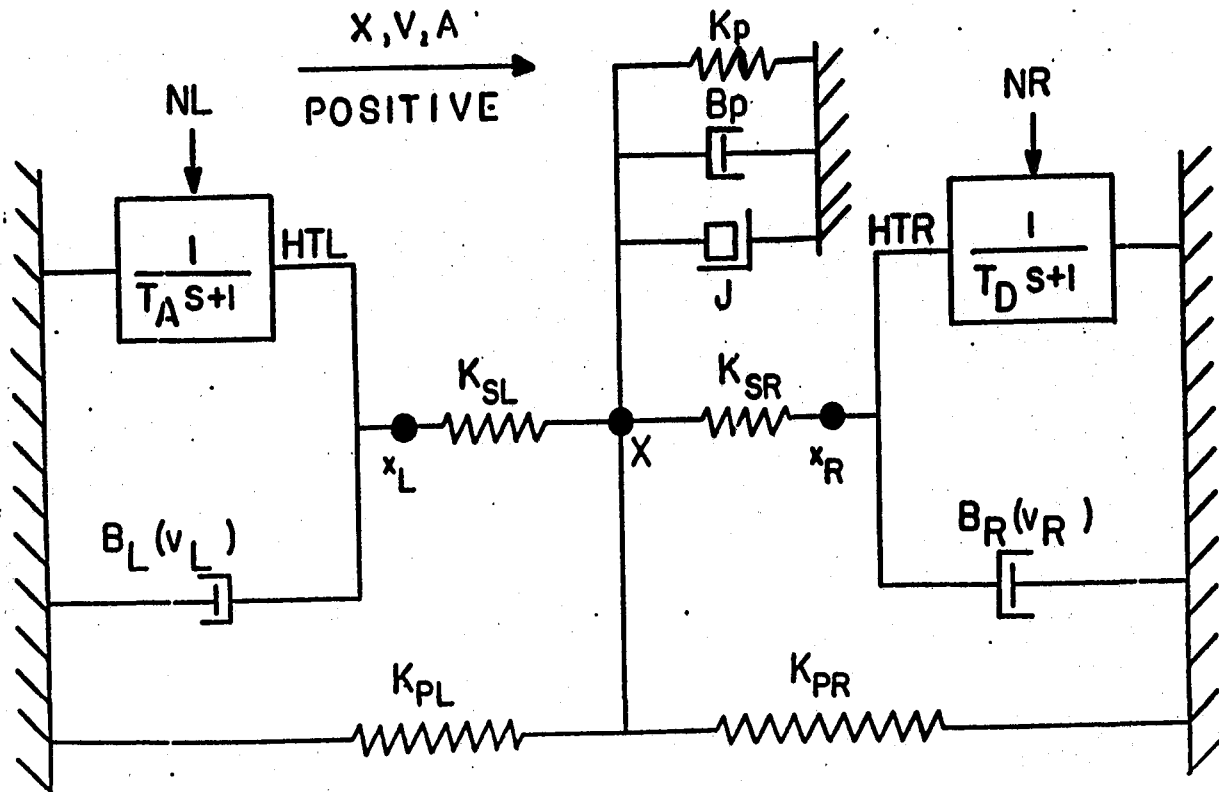


Figure 1

6th Order Non-Linear Model of the head rotation system.

Zangemeister Lehman and Stark (81ab) simulated the muscles and plant of the head movement system with a 6th order non-linear model incorporating Hill's force-velocity relationship, two antagonist muscles, and an overdamped second order plant (Figure 1). Their model matched experimentally measured Main Sequence dynamic peaks when driven by heuristically derived control signals. Versions of this model have had a fruitful history of application to many different physiological systems. Stark (1961) proposed and Atwood et. al. (1961) simulated a two-muscle model for understanding neurological control mechanisms. Cook & Stark (1968), and Clark & Stark (1975) used more detailed versions with appropriate parameter values to model saccadic and other eye movements, and it has been applied to the eyelid in modeling the dynamics of the blink (Kim, et. al. 1984b).

In some cases, it is possible to invert a numerical model and obtain controller signals as a function of dynamics. Cook (1965) linearized the model and obtained a closed form solution to the inverse problem. Recently, Kim, et. al.(84a) has developed an iterative method which has been applied to the non-linear model of the eye-movement system. An adaptation of this technique was used in the present work.

## METHODS

### Experimental

Horizontal head position was measured by a precision potentiometer attached to a bicycle helmet frame worn by the subject. To allow for vertical head movement and subjects of differing heights, the potentiometer was coupled to the head through a compliant fitting which unfortunately resulted in a delay of about 50 ms. between actual and recorded head position.

Electromyographic activity was measured differentially with two S&W number 737 self-adhesive Ag-AgCl disposable electrodes placed approximately 5cm apart on the skin along the major axes of the left and right splenius capitus muscles. EMG and position data was digitized at 1000 Hz by an LSI 11-23 computer with 12 bit analog to digital converters (Hannaford et.al. 1983).

The subject's head movements were made in response to light emitting diode (LED) targets alternately flashing at points on a curved screen 1 meter from the subject's head. The subject was aware of the exact position of his head by a small spot of light projected from his helmet onto the screen. When the target illumination alternated between the two positions, (at intervals of 4 seconds) the subject performed 20, 40, and 60 degree horizontal head movements.

The subjects were instructed to move their heads "as fast as possible" to produce an intent to respond to the target in a time-optimal manner. This experiment resulted in stereotyped movements which could be ensemble averaged along with their

rectified EMGs.

In a separate experiment, the targets were set 40 degrees apart and the subject was given different instructions for movements in the two different directions. For movements to the right, the subject was asked to make time-optimal movements as in the first experiments. For the leftward movements, he was instructed to move "however you want." Of the many and varied leftward movements that resulted from this paradigm, two leftward movements occurring directly after each other (with one time-optimal rightward movement between them) were selected for analysis.

### Modeling

For simulation of the horizontal head rotation system, we used the sixth-order non-linear model developed by Zangemeister, Lehman, and Stark (1981ab). This model consists of two identical, antagonistic muscle elements driving a second order plant (Figure 1). The muscle elements have a force generator driven through a first order low pass filter representing the calcium activation process. The control signals,  $n_l$  and  $n_r$ , range from zero to one to represent the possible range of excitation from none to full excitation. To help the reader's intuition, we have plotted this signal in equivalent kilograms to suggest the steady state force that would result from constant excitation at a given level. In parallel with the force generator is a non-linear viscous element representing the Hill's force-velocity relationship (Hill, 1938). Force is transmitted to the load through a series elastic element representing the properties of muscle tendon and attached cross-bridges.

This system is modeled and simulated by a set of 6 state equations and two ancillary equations (Table 1). The values used for the parameters (Table 2) are based on previous work (Zangemeister, Lehman & Stark, 1981a) and recent, improved estimates (J.M. Winters, private communication).

State Equations

$$\begin{aligned} \dot{x} &= v \\ v_l &= (htl - ks(xl-x)) / b_l \\ v_r &= (-htr - ks(xr-x)) / b_r \\ a &= (-k_p x - b_p v + ks(xl - x) + ks(xr - x)) / j \\ dh_{tl} &= (n_l - h_{tl}) / t_a \\ dh_{tr} &= (n_r - h_{tr}) / t_a \end{aligned}$$

Ancillary Equations

$$\begin{aligned} b_l &= \begin{array}{l} (1.25 h_{tl}) / (b_h + v_l) \\ 1.25 h_{tl} / 900. \end{array} & \begin{array}{l} v_l > 0 \\ v_l < 0 \end{array} \\ b_r &= \begin{array}{l} (1.25 h_{tr}) / (b_h + v_r) \\ 1.25 h_{tr} / 900. \end{array} & \begin{array}{l} v_r < 0 \\ v_l > 0 \end{array} \end{aligned}$$

TABLE 1  
Equations for the sixth order non-linear model  
of horizontal head rotation.

- - -

Name	Symbol	Value	Units
Parallel Viscosity	b <sub>p</sub>	2.0	gr-f deg <sup>-1</sup> sec
Activation Time Const.	t <sub>a</sub>	50.0	milli seconds
Hill's Constant; b	b <sub>h</sub>	350.0	deg sec <sup>-1</sup>
Rotational Inertia	j	0.18	gr-f deg <sup>-1</sup> sec <sup>2</sup>
Series Elasticity	k <sub>s</sub>	350.0	gr-f deg <sup>-1</sup>
Parallel Elasticity	k <sub>p</sub>	2.0	gr-f deg <sup>-1</sup>

TABLE 2  
Model Parameter Values.

Inversion by Iteration of Forward Model

The simulations typically undertaken with such a model involve applying various control signals at the model's inputs (the neurological force commands to the muscles, n<sub>l</sub> and n<sub>r</sub>, are presumably a product of firing rate and recruitment) and observing the model's output; position, velocity, and acceleration time functions. In this study, we reversed the process, obtaining the control signal as a function of experimentally recorded movement dynamics.

To do this, we used an iterative method which, at each time sample, involves finding the control signal values which result in model output that exactly matches the experimentally recorded

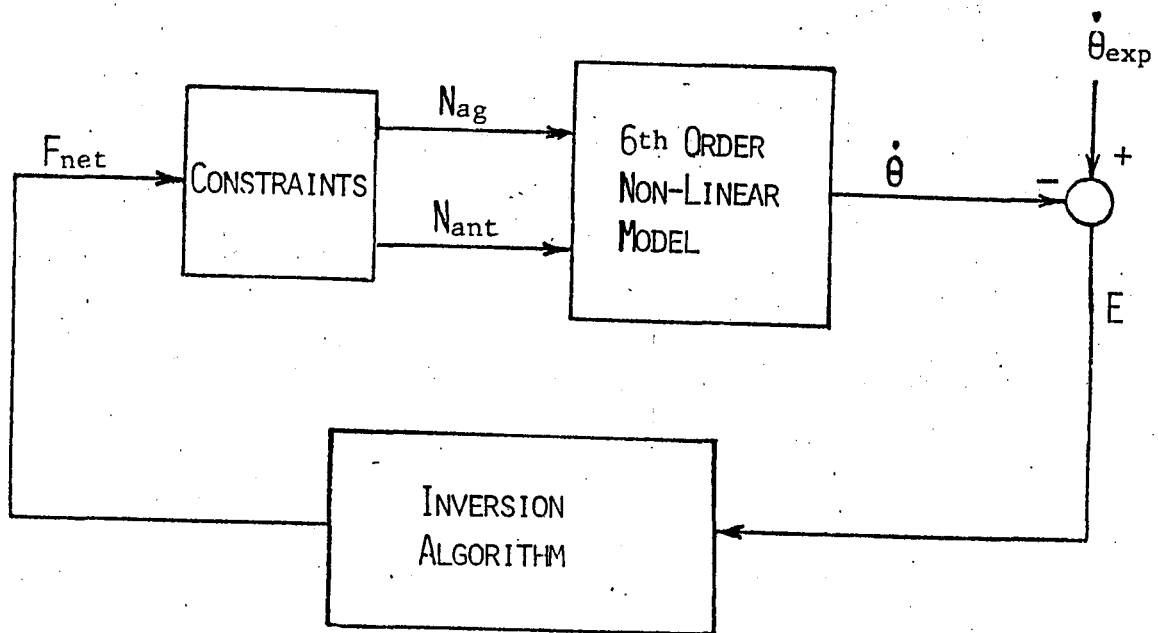


Figure 2

Block diagram of iterative model inversion process.

dynamics at that time (Figure 2). When these control signal values are obtained, the state variables are updated and the process is repeated for the next time sample. Several issues arise which must be resolved before this computation can be performed.

Because the system has only one measurable output, head position, only one independent variable can be obtained by inversion of the model. In order to use an iterative method to minimize the difference between model output and experimental data, the two model inputs, agonist and antagonist control signals must be constrained to be a function of this single variable. In these simulations, the independent variable was net force (fnet) and the constraint used was:

$$\begin{array}{ll} f_{\text{agonist}} & = f_{\text{min}} + f_{\text{net}} & f_{\text{net}} > 0 \\ f_{\text{antagonist}} & = f_{\text{min}} \\ \\ f_{\text{agonist}} & = f_{\text{min}} & f_{\text{net}} \leq 0 \\ f_{\text{antagonist}} & = f_{\text{min}} + f_{\text{net}} \end{array}$$

where fnet = 80 grams-force (the small, minimal force level, fmin in each muscle is necessary for stability of the simulation). Although this constraint does not allow co-contraction, that is simultaneous activation of both muscles, other constraints are possible which do. This constraint was suggested by the absence of co-contraction shown in the EMG recordings we analyzed.

### Iteration Methods

With net force driving the model through the constraints and generating agonist and antagonist force commands, the problem becomes to find the value of net force for which

$$E = 0$$

where

$$E = V_h(t) - V_m(t, f_{\text{net}})$$

and  $V_h(t)$  is head velocity as a function of time over ( $0 < t < t_{\text{max}}$ ), and  $V_m(t, f_{\text{net}})$  is the model output as a function of fnet and its previous values. Solving this equation for each value of t from 0 to tmax yields net force as a function of time. By applying the constraint, we then have agonist and antagonist force control signal as a function of time.

The method initially used to solve this equation at each time sample was an adaptation of the Newton-Raphson method in which fnet was iterated until the value of E was less than a small epsilon. After E was calculated for two values of fnet, the new estimate for fnet is

$$fnet_{j+1} = \frac{E_{j-1}f_j - E_j f_{j-1}}{E_{j-1} - E_j}$$

where  $j$  is the iteration number.

Although this method was effective, it occasionally failed to converge when  $V_m(t, fnet)$  was sufficiently non-linear as a function of  $fnet$ . It was subsequently found that a binary search method would guarantee convergence of the algorithm.

In this second method, an initial range of values is selected between which it is assumed must lie the correct value of  $fnet$ . This range can easily be determined by taking the maximum expected force value and allowing  $fnet$  to vary between that value both above and below zero. The first estimate in this procedure is zero. Then each subsequent estimate is improved by an increment equal to the maximum value divided by a larger and larger power of two. If the value of  $E$  resulting from this new estimate of  $fnet$  is negative, the next increment is subtracted from  $fnet$ . If it is positive, it is added. Convergence relies on the assumption that  $E$  crosses zero at least once at some value of  $fnet$  between the initial guesses, an assumption which can always be made true by widening the initial range at a slight expense in convergence time.

### Numerical precision

Compared to the eye movement system (Kim et al, 1984a), the head movement system has very long time constants; a step change in controller signal results in a very small instantaneous change in head velocity. Also, small amounts of noise, including quantization noise, in the velocity signal will require large changes in the control signal in order for the model output to match this noise. Thus attention must be paid to numerical precision and filtering if this calculation is to be successful. In our computations, we used double precision arithmetic for all calculations of state variables, ancillary equations, and system error,  $E$ . Furthermore, we filtered the input data to produce a double precision result with a sufficiently small amount of noise and quantization error. Filtering did not result in appreciable changes in movement dynamics.

### Filtering and Effects of Bandwidth

Filtering of head movement trajectories was necessary to reduce undesired measurement and quantization noise. For this smoothing operation, a Hamming window, zero-phase-delay, low pass filter was used (Rabiner & Gold, 1975). The frequency response of the ideal low pass filter is

$$H(jw) = \begin{cases} 1 & \text{for } -w_c < w < w_c \\ 0 & \text{elsewhere} \end{cases}$$

where  $w_c$  is the desired cutoff frequency. The filter we used is

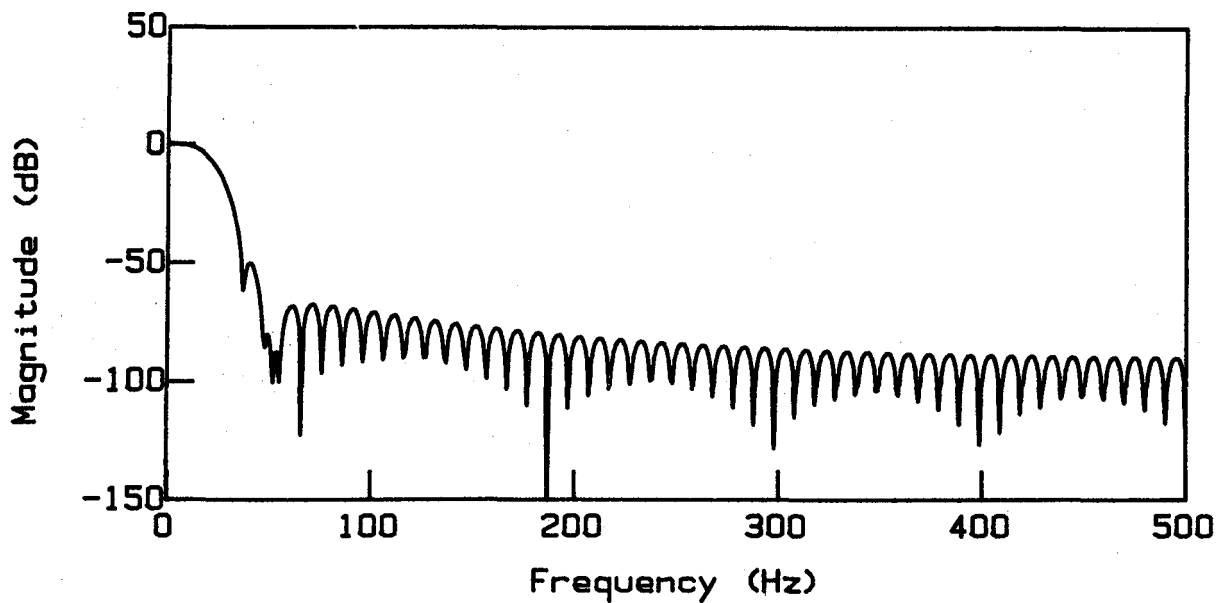
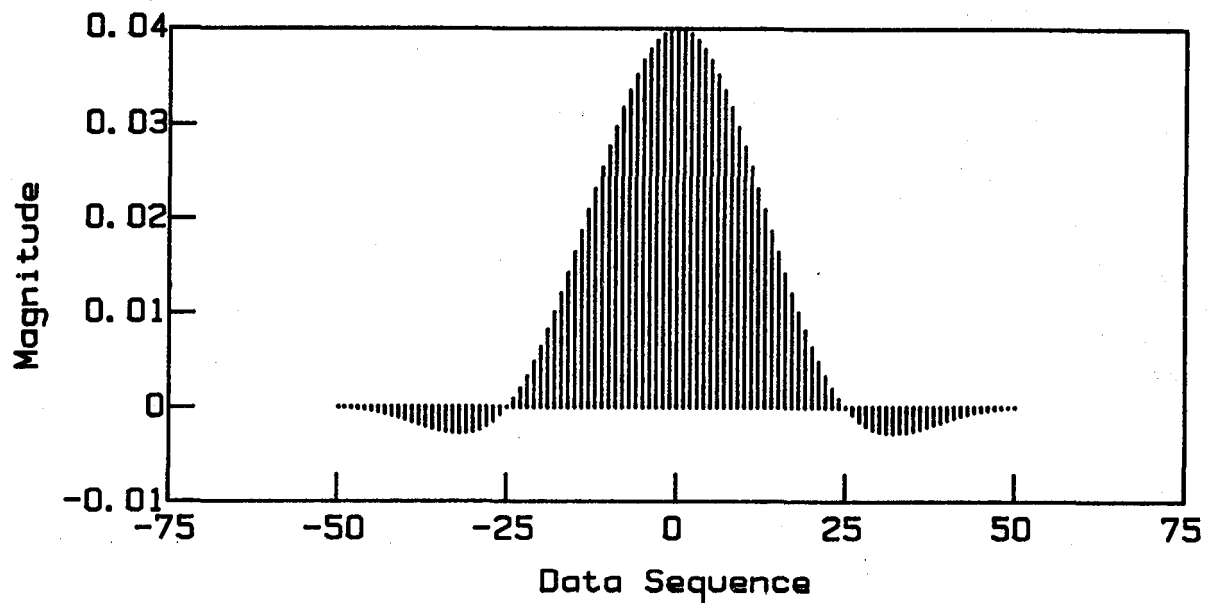


Figure 3

Smoothing of movement dynamics necessary for model inversion was performed with a 100 point Hamming window low pass filter. Impulse response of this filter (top) is symmetrical about zero to eliminate phase delay. Frequency response (bottom) shows sharp cutoff at 20 Hz.

one which comes close to this ideal response. The impulse response of the ideal low pass filter is

$$h(n) = \frac{\sin \frac{n \omega_c}{\omega_s}}{\pi n}$$

where  $\omega_s$  is the sampling frequency. The ideal impulse response extends to infinite values of  $n$ . The Hamming window is employed as a finite weighting sequence on the infinite ideal impulse response to produce smooth truncation. The weighting function of the Hamming window is

$$w(n) = 0.54 + 0.46 \cos(2\pi n / N), \quad -N \leq n \leq N$$

where  $N$  is the number of data points for the truncation window. The modified impulse response weighted by the Hamming window is

$$hw(n) = h(n) \cdot w(n).$$

The output sequence  $y(n)$  of the Hamming window low pass filter is given by the convolution of the input sequence with the modified impulse response  $hw(n)$ . Note that  $hw(n)$  is symmetrical with respect to  $hw(0)$ . The filtered output sequence  $y(n)$  can thus be described by a finite difference equation as;

$$y(n) = hw(0) x(n) + hw(1) (x(n-1)+x(n+1)) + hw(2) (x(n-2)+x(n+2)) + \dots$$

For smoothing the position and velocity trajectories, we used a Hamming window low pass filter of 100 data point with a cutoff frequency of 20 Hz at a sampling rate of 1000 Hz (Figure 3).

## RESULTS

### Time Optimal Movements

We prepared 3 ensemble averages of fast movements at amplitudes of 20, 40 and 60 degrees ( $n = 5$ ). Velocity and acceleration traces show amplitude-dependent peak values characteristic of time-optimal movements (Figure 4). Full-wave-rectified EMG activity from agonist and antagonist muscles was also averaged (Figure 5). The EMGs exhibit the tri-phasic burst pattern found in fast movements about several different joints (Wachtolder, Angel, Ghez & Martin, Litvintsev & Seropyan, Wadman, van der Gon, & Derksen, Hannaford et. al., 83, Cheron & Godaux). It is difficult to quantify signals of this type in terms of height and width. However, as a function of movement magnitude, they seem to vary more in width than in amplitude although PA, the first

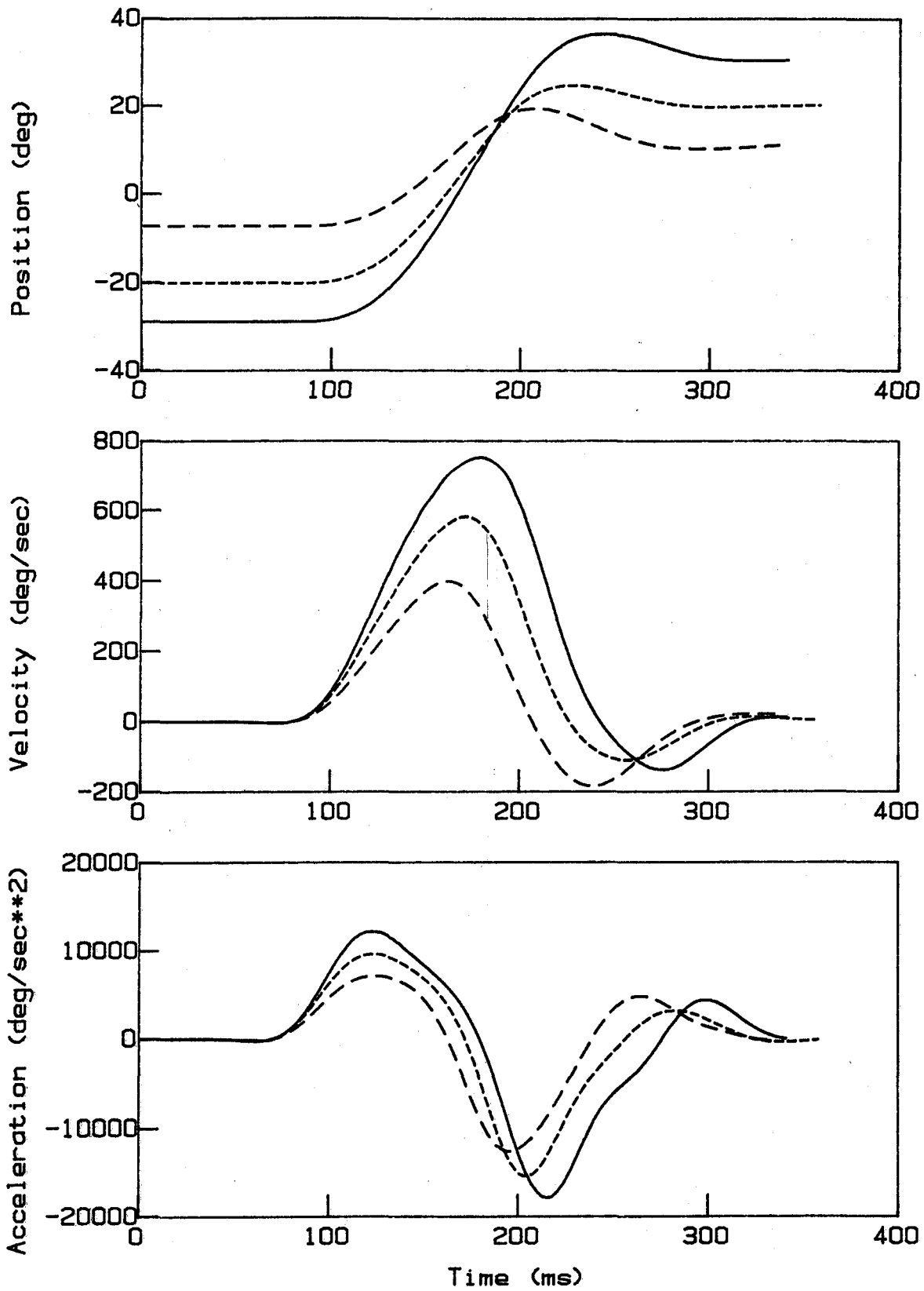


Figure 4

Three ensemble averages of time-optimal horizontal head movements of 20, 40, and 60 deg. (n=5). Also shown are velocity (middle) and acceleration (bottom) computed from the filtered data.

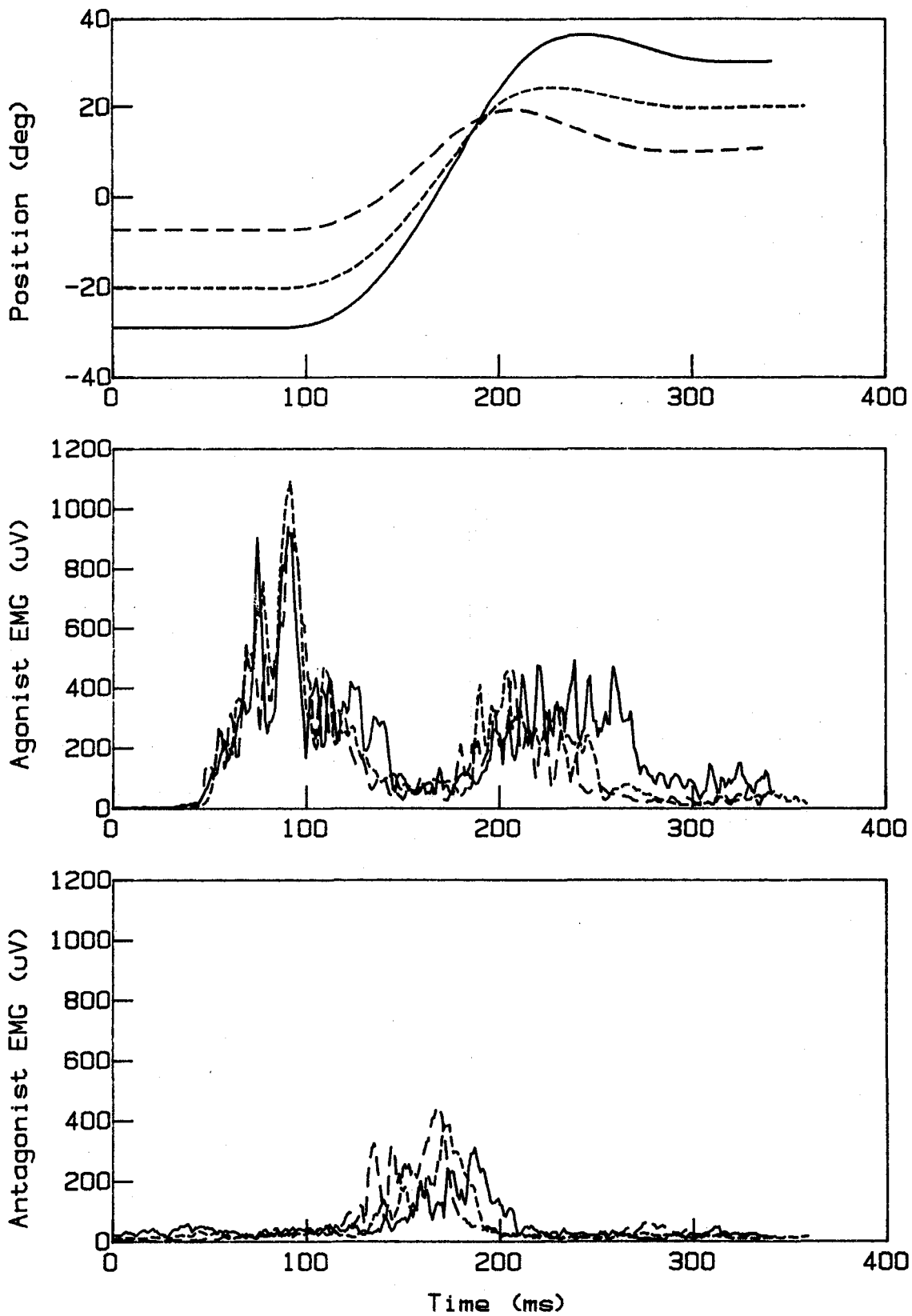


Figure 5

Rectified and averaged EMG's, taken from left and right splenius capitus muscles, during same time-optimal movements as in figure 4.

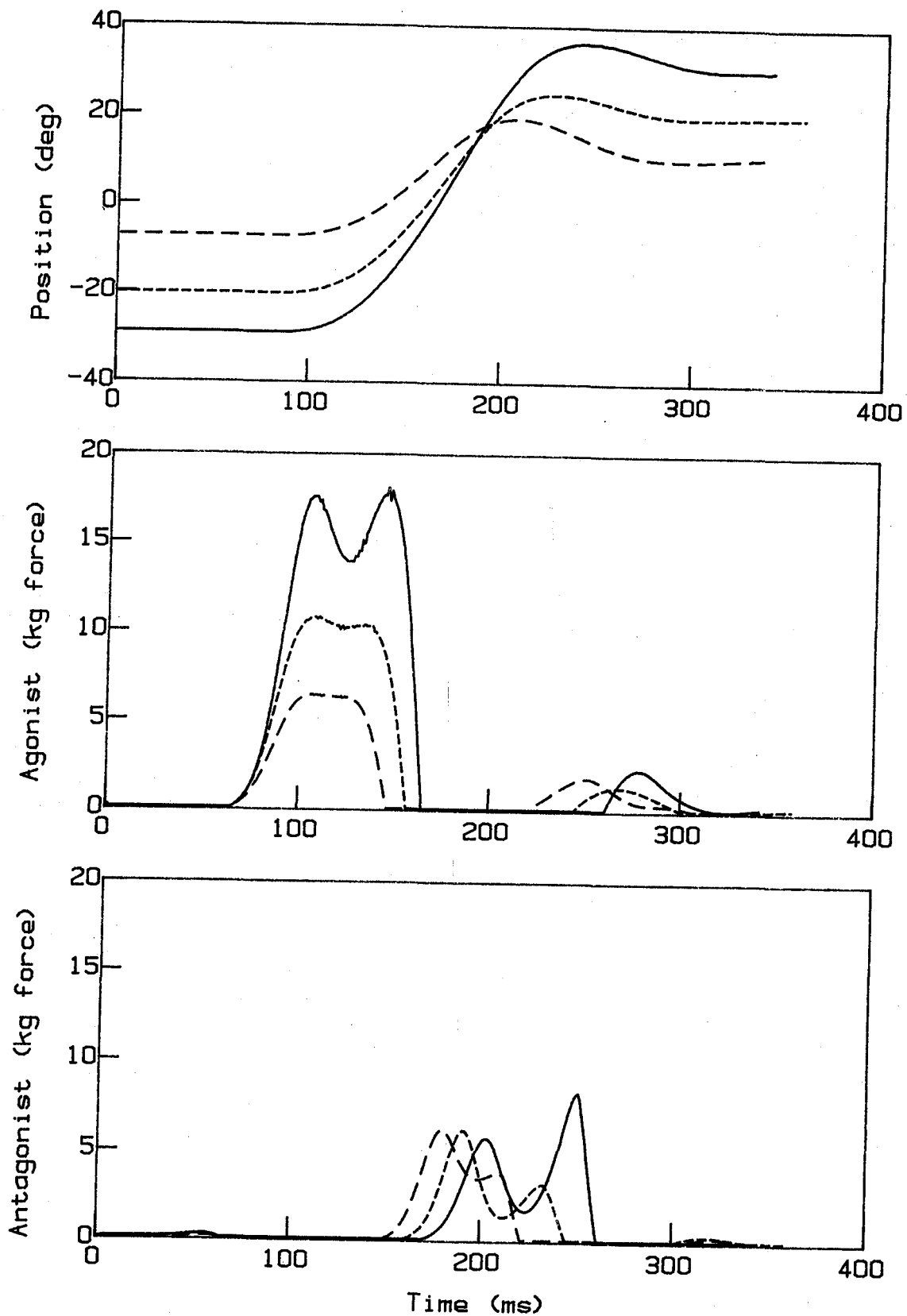


Figure 6

Controller signals obtained by inverse modelling of the three time optimal movements of figures 4 and 5. Three pulses of excitation are seen which correspond to the three EMG pulses

agonist EMG burst reaches a peak value about twice that of PB and PC.

The result of the inverse modelling process is a pair of control signals describing the excitation levels of the antagonistic muscle pair for each of the three movement magnitudes. This signal (Figure 6) also shows the tri-phasic pattern, having an initial agonist burst followed by a burst of antagonist activity and finally a second antagonist burst. PA, the first agonist pulse, increases from 75 to 100 ms in width and from 6 to 17 equivalent kilograms (kge) in amplitude as movement magnitude increases from 20 to 60 degrees. PB ranges from 70 to 100 ms in width and has a relatively constant amplitude of about 6kge except for a second peak of about 8 kge in the 60 degree case. PC appears to be fairly constant at about 40 ms in width and about 2 kge in amplitude. The skew evident in PB and PC is due to the concatenation of the three pulses; as longer pulses are concatenated, later pulses are delayed appropriately.

Comparison of the EMG records with controller signals resulting from the inversion shows a delay of about 30 ms. between EMG and control signal resulting from delay in the head position measurement apparatus not accounted for in the model. The width of PA, the first agonist EMG burst matches well with the first agonist control signal pulse for all three magnitudes. The antagonist excitation pulse shows the same increase in onset times (of roughly 10 ms./20deg) with movement magnitude as does PB, the antagonist EMG burst. But each antagonist control signal pulse is longer than the corresponding EMG pulse. While the EMG pulse, PA is of roughly constant amplitude, the first control signal pulse amplitude varies over a three to one range with movement magnitude.

PC, the second agonist EMG burst, is of roughly constant amplitude but its width varies strongly with movement magnitude from about 60 to 75 ms. Width of the third control signal pulse is difficult to ascertain because of its approximately exponential decay, but unlike the PC of the EMG, its amplitude is quite small relative to the first pulse at all three magnitudes. A hypothetical linear relationship between EMG magnitude and control signal magnitude would suggest that the third control signal pulse have an amplitude roughly half of that of PA but in fact, it is much less. This may suggest that the model is too viscous during the later phase of the movement, requiring less active damping than does the real system.

### **A Pair of Slow Movements**

Figure seven depicts two double movements. These single records (not averages) were taken of the subject on successive leftward rotations under instructions to move "however you want to". Both records begin with a movement of approximately 15 degrees to the left which is of insufficient amplitude to reach the target. The peak velocity of this movement was 210 deg/sec for the solid and 220 deg/sec for the dashed record. A second deflection of the

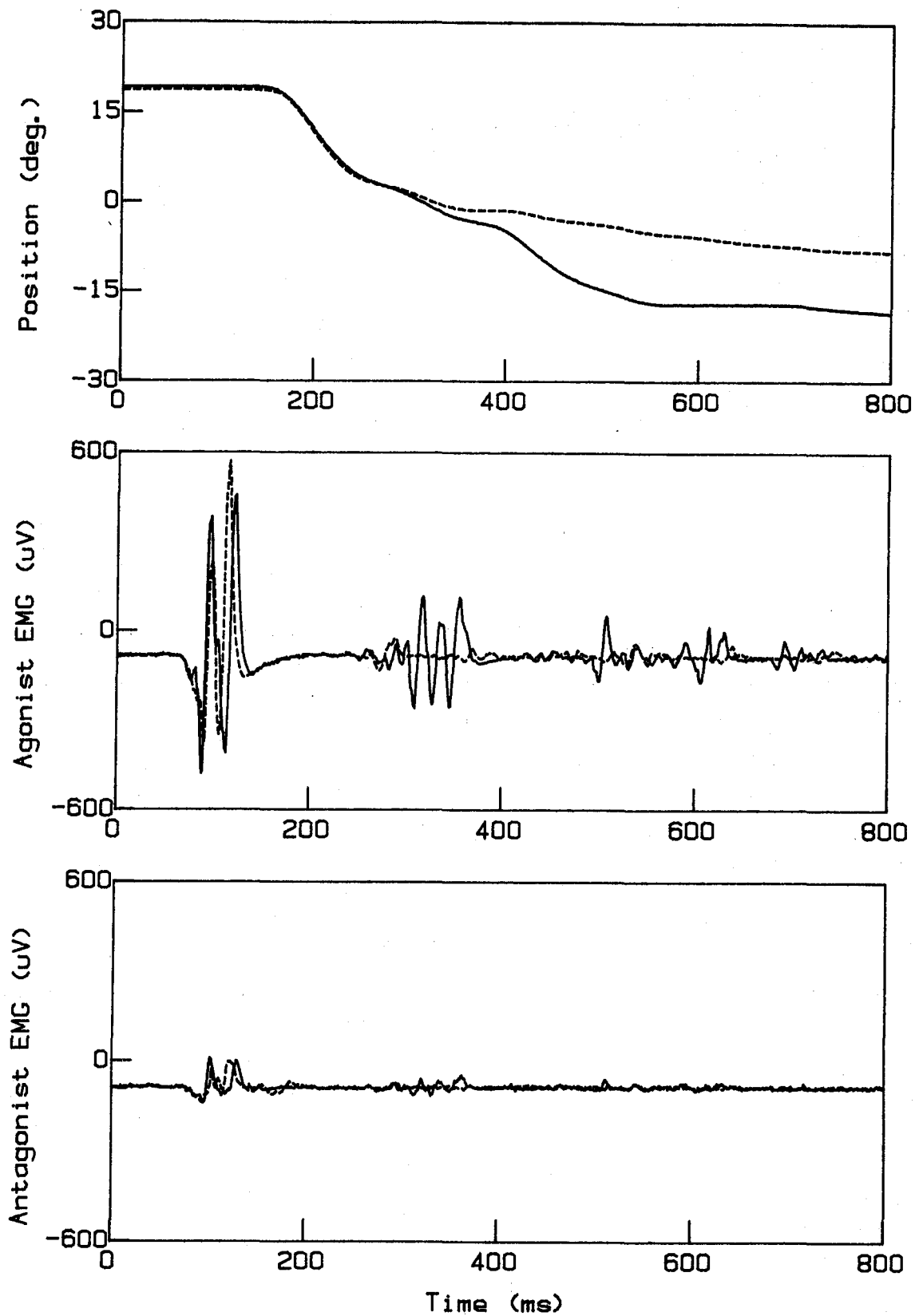


Figure 7

Records of two double movements and their EMG's. First movement is nearly identical in both records while a second, corrective, movement appears in the later record (solid trace) about 240 ms. after the first. Note similarity in duration, amplitude and number of pulses of EMG bursts causing first movement, and divergence of EMG's as dynamics diverge.

position trace appears about 100 ms. later. About 220 ms after the first movement, the subject made a second, corrective movement to cover the remaining distance. The solid record makes a discrete corrective movement of about 15 deg. with a velocity peak of 135 deg/sec. In the dashed trace, there is instead a drift at an approximately constant velocity of about 20 deg/sec. The first movement is nearly the same in both records while the second movement is of larger amplitude and velocity in the second of the two records (solid trace).

An initial burst of agonist EMG is seen in both records. These bursts are similar in amplitude, duration, and number of spikes. The antagonist channel shows a small amount of EMG activity due to either cross-talk or a small amount of co-contraction. No antagonist EMG activity appears after the initial agonist burst (PA). The second EMG burst is much more prominent in the second record (solid) and the corresponding second movement is greater.

Control signals were calculated using the inverse model on the velocity trajectories of the two records (Figure 8). The calculated control signals consist of a series of rounded, roughly triangular pulses, the first and largest ones resulting from the initial movement in both records. These pulses have a peak force value of about 5 kge. with the dashed pulse slightly greater corresponding to the slightly greater peak velocity. Both pulses are about 60 ms in duration. The slight difference in peak force corresponds to the slightly faster time course of the first movement in the first record (dashed lines). The control signal obtained by the inversion contains 6 subsequent, smaller, pulses of activity in the agonist and 6 in the antagonist.

The second agonist pulse (about 1 kge peak force, and about 50 ms duration) corresponds to the slight increase in velocity seen about 100 ms. before the start the second movement. 220 ms after the initial agonist burst, the second movement is initiated by another burst of agonist activity. Here, as the dynamics diverge between the two records, a larger agonist burst (3 kge vs less than 1 kge peak force and 60 ms vs 50 ms pulse width) appears in the later (solid) record corresponding to the larger movement.

Small pulses of antagonist force follow immediately after each agonist pulse and immediately precede the next agonist pulse. These pulses are not present in the EMG records and their presence may be due to the fact that the filtering of the dynamics results in slight dynamical changes requiring a smoothly changing or "ringing" control signal. Another possibility is that since no co-contraction is possible because of the control signal constraint, active damping may be required of the control signal to make up for lack of an active viscosity due to co-contraction but no co-contraction is evident in the EMG. Finally, it may be that other neck muscles such as the left and right sterno cleido mastoid may be activated at these times. Recording of additional EMG channels may clarify this possibility.

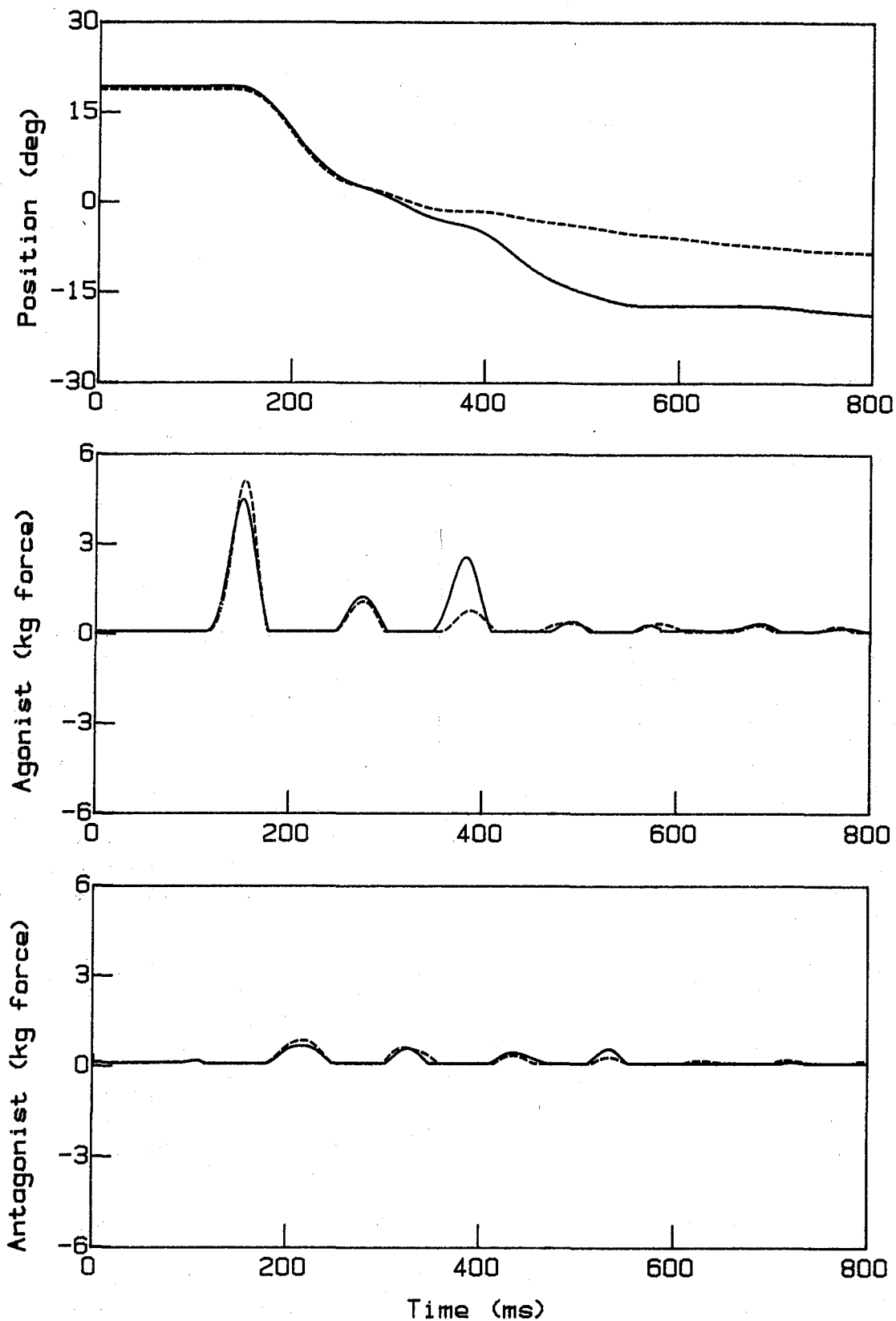


Figure 8

Control signals obtained by inverse modelling of two slow movements shown in figure 7. Timing shift between EMG's (fig. 7) and control signal pulses (this fig.) is due to time delay in experimental apparatus. Extra pulses of controller signal activity may be due to lack of co-contraction imposed by controller signal constraint, or activity of other neck muscles, not recorded in fig. 7.

## DISCUSSION

Inversion of the head model is an interesting problem in numerical analysis. Because of the long time lags involved, the problem is near to being ill conditioned (Rice, 1984). Use of FORTRAN's double precision arithmetic was required both for the computation of state variables and for the results of the data filtering against which model output was matched.

Algorithms for solving for a zero of the output error function  $E$  must be sufficiently able to deal with the non-linear behavior of the model to guarantee convergence in a reasonable amount of time. A binary search algorithm was found to always converge but to take more time, in many cases, than a successive approximation method based on the Newton-Raphson algorithm. A suitable improvement would be a successive approximation method generating a rough estimated range, followed by a binary search to guarantee convergence and full double precision accuracy.

Another area for further study is that of the controller signal constraints by which net force is converted to agonist and antagonist control signals. The constraint used in this study was suggested by the fact that appreciable co-contraction was not evident in the EMG records from time-optimal movements. Cook (1965) and Kim, et.al. (1984a) in inverting the eye movement system have used another possible constraint, which specifies a given amount of co-contraction in terms of a ratio of antagonist to agonist excitation. For example, if the co-activation level is set to 20%, and the excitation level required is 1, then the agonist would be set to 1 and the antagonist to 0.2. It will be interesting to recompute the above results with this type of constraint and assess the effect of co-contraction level on antagonist activity in the slow movements.

The inverse modeling process is an aid to understanding the control of skeletal muscle in movements and helps create a conceptual link between EMG and movement dynamics. Completion of this link will yield the ability to predict movement dynamics from a knowledge of the plant and of the EMG signal. The three unresolved steps in this link are the calibration of EMG to excitation; the improvement of experimental apparatus to reduce delays, non-linearities, and frequency dependent effects; and the further elaboration of the subtle non-linearities in the model.

The above process of "Dynamic Calibration" would be a step toward an ideal EMG signal processor in the sense that the response of the Hamming window low pass filter approaches that of the ideal low pass filter. So far, the only signal processor to adequately interpret the EMG is still the living muscle.

## REFERENCES

1. Angel, R.W., "Myoelectric patterns associated with ballistic movement: effect of unexpected changes in load.", J. Human Movement Studies Vol. 1, p.96-103, 1975
2. Atwood, J., Elkind, J., Houk, J., King, M., & Stark, L. "Digital Computer Simulation of a Neurological System.", Quarterly Progress Report; Research Laboratory of Electronics, MIT, Oct. 15, 1961.
3. Cheron, G., & Godaux, E., "Ballistic Movements in Man: Pre-Programmed Activities and Reflex Influences", Pre-print 5/84
4. Clark, M. & Stark, L. "Time Optimal Behavior of Human Saccadic Eye Movements", IEEE Trans. Automatic Control, Vol AC 20, 1975 p. 345-348
5. Cook, G., "Control Systems Study of the Saccadic Eye Movement Mechanism," PhD Thesis, Department of Electrical Engineering, Mass. Inst. of Technology, 1965.
6. Cook, G., and Stark, L., "The Human Eye Movement Mechanism: Experiments, Modeling, and Model Testing," Archives of Ophthalmology, vol. 79, p428-436, 1968.
7. Ghez, C., & Martin, J.H., "Control of Rapid Limb Movement in the Cat. III. Agonist-Antagonist Coupling." Exp. Brain Research. Vol. 45 pp 115-125, 1982.
8. Hannaford, B., Maduel, R., Nam, M.H., Lakshminarayanan, V., and Stark, L., "Effects of Loads on Time-Optimal Head Movements: EMG, Oblique, and Main Sequence Relationships," Proceedings of the 19th Annual Conference on Manual Control, MIT, June 1983.
9. Hannaford, B., Nam, M.H., Lakshminarayanan, V. & Stark, L., "EMG as Controller Signal with Viscous Load," Journal of Motor Behavior, submitted 5/83 revised 10/83 accepted 11/83.
10. Hill, A.V., "The Heat of Shortening and Dynamic Constraints of Muscle," Proceedings of the Royal Society, London, Vol. 126, pp.136-195, 1938.
11. Kim, W.S., & Stark, L., "Inverse Modeling to Obtain Neurological Control Signals of the Non-Linear Eye Movement Model.", In Progress., 1984a.
12. Kim, W.S., & Stark, L., "Inverse Modeling to Obtain Neurological Control Signal in the Blinking Eye.", In progress. 1984b.
13. Lehman, S.L., & Stark, L., "Perturbation Analysis Applied to Eye, Head, and Arm Movement Models," IEEE Transactions on Systems, Man, and Cybernetics, Sept. 1983.

14. Lehman, S. & Stark, L., "Simulation of Linear and Nonlinear Eye Movement Models: Sensitivity Analysis and Enumeration Studies of Time Optimal Control", J. Cyber. & Inf. Sci. vol. 4
15. Litvintsev, A.I., & Seropyan, N. S., "Muscular Control of Movements with One Degree of Freedom: I Single Movements" Avtomatika i Telemekhanika, no. 5, pp. 88-102, May, 1977
16. Rabiner, L.R., & Gold, B., "Theory and Application of Digital Signal Processing.", Prentice-Hall, Inc. 1975. pp. 75-105
17. Rice, J.R., "Numerical Methods, Software, and Analysis", McGraw Hill, 1983
18. Stark, L., "Neurological Organization of the Control System for Movement.", Quarterly Progress Report #61, Research Laboratory of Electronics. MIT, April 15, 1961. pp. 215-217
19. Wachholder, K., Altenburger, H., "Beitrage zur Physiologie der willkurlichen Bewegung.", 10 Einzelbewegungen Pflugers Arch Ges Physiol Vol. 214, pp 642-661, 1926
20. Wadman, W.J., van der Gon, J.J.D. & Derksen, R.J.A., "Muscle activation patterns for fast goal directed arm movements," J. Hum. Move. Stu., Vol. 6, 1980, p. 19-37.
21. Zangemeister, W. H., & Stark, L., "Dynamics of head movement trajectories: Main Sequence Relationship," Exp. Neuro., Vol. 71, 1981a, p. 76-91.
22. Zangemeister, W. H., Lehman, S., & Stark, L., "Sensitivity analysis and optimization for a head movement model," Biol. Cybern., Vol. 41, 1981b, p. 33-45.
23. Zangemeister, W. H., Lehman, S., & Stark, L., "Simulation of head movement trajectories: model and fit to main sequence," Biol. Cybern., Vol. 41, 1981c, p. 19-32.
24. Zangemeister, W.H. & Stark, L., "Active head rotations and eye head coordination," Annals N.Y. Acad. of Sci., 1981d, p. 540-559.
25. Zangemeister, W. H., Stark, L., Meienberg, O., & Waite, T., "Neurological control of head rotations: electromyographic evidence," J. Neurological Sci., Vol. 55, 1982, p. 1-14.